Am J Transl Res 2014;6(5):528-537
www.ajtr.org /ISSN:1943-8141/AJTR0001326

Original Article

Maytansine-loaded star-shaped folate-core PLA-TPGS nanoparticles enhancing anticancer activity

Xiaolong Tang[1,2*], Hong Dai[3*], Yongxiang Zhu[1,2], Ye Tian[1], Rongbo Zhang[1], Rengbiao Mei[1], Deqiang Li[4]

[1]Stem Cell Engineering Research Center, School of Medicine, Anhui University of Science and Technology, Huainan 232001, P.R. China; [2]The State Key Laboratory of Virology, Life Sciences College, Wuhan University, Wuhan, Hubei 430072, P.R. China; [3]Department of Clinical Laboratory, Medical College, Hunan Normal University, Changsha 410006, Hunan, China; [4]Department of Integrated Internal Medicine, The First Affiliated Hospital of Zhejiang University, Hangzhou 310003, China. [*]Equal contributors.

Received July 6, 2014; Accepted August 20, 2014; Epub October 11, 2014; Published October 15, 2014

Abstract: The efficient delivery of therapeutic molecule agents into target cells of interest is a critical challenge to broad application of non-viral vector systems. In this research, maytansine-loaded star-shaped folate-core polylactide-D-α-tocopheryl polyethylene glycol 1000 succinate (FA-PLA-TPGS) block copolymer was applied to be a vector of maytansine for folate receptor positive (FR^+) breast cancer therapy. The uptake of maytansine nanoparticles by SKBR3 cells were observed by fluorescence microscopy and confocal laser scanning microscopy. The cell viability of maytansine-NPs in SKBR3 cells was assessed according to the changed level of intracellular microtubules and apoptosis-associated proteins. The cytotoxicity of the SKBR3 cells was significantly increased by maytansine-NPs when compared with control groups. In conclusion, the maytansine-NPs offer a considerable potential formulation for FR-expressing tumor targeting biotherapy.

Keywords: Maytansine, targeted delivery, chemotherapy, folate, nanomedicine

Introduction

As the mainstay in the treatment of various cancers for several decades, chemotherapy significantly improved tumor efficacy, improved quality of life and prolong survival of patients. With the development of science and technology, various chemotherapy drugs to treat tumor have been developed [1, 2], in which, maytansine has the most significant clinical efficacy. It is a microtubule-targeted drug that binds to tubulin at the vinca binding site as vinca alkaloids, and depolymerizes microtubules and arrests cells in mitosis [3]. Microtubules are polymers composed of the protein tubulin that play a major role in mitosis and other important cell functions [4]. Many microtubule-targeted compounds, including the vinca alkaloids, suppress dynamic instability, and they do so at concentrations significantly lower than those required to depolymerize microtubules [5, 6]. Suppression of dynamic instability plays a major role in the anti-mitotic effects of these drugs [7]. Significantly, maytansine displays almost 100 times higher cytotoxicity in cells than the vinca alkaloids, but it still faces challenges including non-selectivity and high toxicity. Improving the selectivity is therefore a critical step to improve its therapeutic efficacy.

Nanomedicine, especially drug formulation by polymeric nanoparticles (NPs), has shown a great deal of promise to provide solutions to such problems as improving therapeutic efficacy and reducing systemic toxicity in cancer treatment [8, 9]. Folate (FA) is one of the most commonly used targeting moiety to specifically deliver various therapeutic agents, and nanoscaled systems to tumor cells. FA binds to folate receptor (FR) with a very high affinity (KD 0.1~1 nM) [10, 11]. The FR is over-expressed on the surface of many malignant cells including ovarian, lung, breast, and endometrial cancers [10, 11]. The expression of FR on other normal tissues is very low and only restricted to some epithelial cells, and FA has a low immunogenicity and relatively simple chemistry compared to other targeting moieties such as antibody, pep-

tide and aptamer, which make these tumors as excellent candidates for molecular targeting through the folate receptor system. The d-α-tocopheryl polyethylene glycol 1000 succinate-poly (D,L-lactide-co-glycolide) (PLA-TPGS)-based nanoparticles have been studied as delivery vehicles of drugs in our previous research [12]. In recent years, branched polymers, specifically star-shaped polymers and dendrimers have obtained great attention due to their useful mechanical and rheological properties for owning a smaller hydrodynamic radius, lower solution viscosity, higher drug loading capacity and higher drug entrapment efficiency. Moreover, the existence of FA moiety in biomaterials could also significantly increase both cell targeting and cell adherence [12, 13].

In this research, the star-shaped block copolymer FA-PLA-TPGS was prepared and used for developing a superior nanoparticle carrier of anticancer agent maytansine with satisfactory drug content and entrapment efficiency for breast cancer treatment. The maytansine-loaded FA-PLA-TPGS NPs (maytansine-NPs) as a model drug were characterized and the anticancer effect of nanoparticles was evaluated both *in vitro.*

Materials and methods

Materials

All chemicals and materials were purchased from Sigma (St. Louis, MO) unless otherwise noted. Antibodies against caspase-3, -8 and -9 were obtained from Cell Signaling Technology (Beverly, MA) and the antibodies against Bcl-2 were from Santa Cruz Biotechnology (Santa Cruz, CA). Human breast adenocarcinoma cell line SKBR3 (HER2-over expression) was obtained from American Type Culture Collection (ATCC; Rockville, MD, USA). All chromatographic solvents were of high-performance liquid chromatography (HPLC)-grade quality, and all other chemicals used were of the highest grade commercially available. FA-PLA-TPGS copolymer (M_w approximately 23,000) and PLA-TPGS (M_w approximately 23,000) copolymer were obtained from the Graduate School at Shenzhen, Tsinghua University. Anti-CD20 antibody (Rituximab) was purchased from Adallen Pharma Ltd. Maytansine was prepared as described previously [14] and stored as aliquots of 1 mM stock solutions in DMSO at -70°C.

Fabrication of maytansine-loaded nanoparticles

A modified nanoprecipitation method was used to entrap maytansine into the FA-PLA-TPGS NPs [9, 15]. Briefly, a pre-weighed amount of maytansine drug powder and 100 mg of FA-PLA-TPGS copolymer were dissolved in 8 ml of acetone by vortexing and sonication. The resulting nanoparticle suspension was then stirred at room temperature overnight to remove acetone completely. The nanoparticle suspension was centrifuged at 25,000 rpm for 15 min and then washed 2-3 times to remove the emulsifier and unloaded drug. This mixture was dropwise added into 100 mL 0.03% TPGS aqueous solution under stirring. In the end, the dispersion was lyophilized 48 hours for further use. Nanoparticles used as a control couramin 6-loaded star FA-PLA-TPGS NPs (couramin 6-NPs) and anti-CD20 antibody-loaded star FA-PLA-TPGS NPs (anti-CD20-NPs) were fabricated in a similar manner.

Characterization of maytansine-loaded nanoparticles

Size, surface charge and morphology of the nanoparticles: Before measurement, Freeze-dried nanoparticles were appropriately diluted. The nanoparticle size and zeta potential were determined by Malvern Mastersizer 2000 (Zetasizer Nano ZS90, Malvern Instruments Ltd., UK). All measurements were measured at room temperature after equilibration for 10 min. Average size and zeta potential of different NPs were analyzed using a dynamic light-scattering detector (Zeta sizer ZS90, Malvern, Worcestershire, UK). The data were obtained with the average of three measurements.

The surface morphology of nanoparticles was examined by a field emission scanning electron microscopy (FESEM, JEOL JSM-6301F, Tokyo, Japan). To prepare samples for FESEM, the nanoparticles were fixed on the stub by a double-sided sticky tape and then coated with a platinum layer by JFC-1300 automatic fine platinum coater (JEOL, Tokyo, Japan). Morphological examination of FA-PLA-TPGS nanoparticles (NPs) was performed using transmission electron microscopy (H600, Hitachi, Tokyo, Japan).

Drug content and entrapment efficiency: To determine the contents of drug loading (LC) and entrapment efficiency (EE) of the maytansine-NPs, a predetermined amount of nanoparticles were dissolved in 1 mL methylene dichloride under vigorous vortexing. The solution was transferred to 5 ml of mobile phase consisting of acetonitrile and deionized water (50:50, v/v). A nitrogen stream was introduced to evaporate the methylene dichloride for approximately 20 min, and then a clear solution was obtained for high-performance liquid chromatography (HPLC) analysis (LC 1200, Agilent Technologies, Santa Clara, CA, USA). A reverse-phase C_{18} column (250 mm×4.6 mm, 5 μm, C_{18}, Agilent Technologies, CA, USA) was used at 25°C. The flow rate of mobile phase was 1 mL/min. The column effluent was detected using a UV detector at λ_{max} of 227 nm. The measurement was performed in triplicate. Drug loading and encapsulation efficiency of the drug-loaded nanoparticles were calculated according to the following equations, respectively. Briefly, 10 mg of maytansine-NPs were introduced into Eppendorf tubes and dissolved in 1 mL acetonitrile and diluted by 0.1 M citric acid. Meanwhile, the amount of maytansine in the solution was determined by HPLC.

Drug release assay study: The in vitro release profile of maytansine from maytansine-NPs was determined by measuring the residual amount of maytansine present in the nanoparticles [16]. In brief, 5 mg of accurately weighted lyophilized nanoparticles (maytansine-NPs) were put into a centrifuge tube and redispersed in 8 ml phosphate buffer solution (PBS, containing 0.1% w/v Tween 80, pH 7.4). The tube was put into an orbital shaker water bath and vibrated at 130 rpm at 37°C. At certain time intervals, the tube was taken out and centrifuged at 25,000 rpm for 15 min. The supernatant was then transferred into a glass test tube for HPLC analysis. The pellet was resuspended in 8 mL fresh PBS buffer and put back into the shaker bath for subsequent determination. The accumulative release of maytansine from nanoparticles was plotted against time.

Evaluation of the biological function of maytansine-NPs

Cellular uptake of maytansine-NPs: In this research, coumarin 6 served as a model control molecule, which can be entrapped in star-shaped FA-PLA-TPGS NPs for qualitative and quantitative studying on cellular uptake by tumor cells such as SKBR3 cells. Tumor cells were cultured in Dulbecco's modified essential medium (DMEM) supplemented with 10% heat-inactivated fetal bovine serum and antibiotics (FCS). The cells were incubated with 250 nmol/L coumarin 6-NPs at 37°C for determined time (12 hrs, 24 hrs and 36 hrs) rinsed with cold PBS solution 3 times, and then fixed by methanol for 25 min. Cells were stained with 4'-6'-diamino-2-phenylindole (DAPI) for 30 min to display the nuclei and rinsed twice with PBS solution [9, 17]. Tumor cells were observed by using Confocal laser scanning microscopy (CLSM; LSM 410, Zeiss, Jena, Germany) with an imaging software.

In vitro cytotoxicity of maytansine-NPs: Tumor SKBR3 cells were seeded in 96-well plates at the density of 5×10^3 viable cells per well in 100 μl of culture medium and incubated overnight. The cells were then treated with various concentrations ranging from 0.001 to 10.0 nmol/L of maytansine, star-shaped maytansine-FA-PLA-TPGS NPs (maytansine-NPs) suspension for 48 and 72 h at 37°C in a CO2 incubator. At certain time intervals, the nanoparticles were replaced with the DMEM containing MTT (5.0 mg/mL) and cells were then incubated for additional 4 h. MTT was aspirated off and DMSO was added to each well to solubilize the formazan crystals formed in viable cells. The absorbance of each well was recorded at 570 nm using a 96-well microplate reader. Viability of untreated cells was set at 100%, and absorbance of wells with medium and without cells was set as zero. All of the results were from at least triplicate experiments. The inhibitory concentration IC_{50}, the drug concentration at which cell growth was inhibited by 50% relative to untreated control cells, was calculated by curve fitting of the cell viability versus drug concentration data [18].

Immunofluorescence microscopy

Cells were seeded on coverslips as above and incubated with maytansinoid for 24 h, fixed with 3.7% formaldehyde, and microtubules were stained with mouse monoclonal α-tubulin antibody (DM1A, Sigma-Aldrich, USA) and FITC-conjugated goat anti-mouse antibody (Cappel

Table 1. Characterization of MAYTANSINE-loaded nanoparticles

Polymer	Particle Size (nm)	PDI	ZP (mV)	LC (%)	EE (%)
PLA	136.7±4.1	0.272	-22.8±3.5	8.22	75.71
PLA-TPGS	125.3±3.5	0.193	-19.4±2.7	8.57	83.12
FA-PLA-TPGS	121.4±3.3	0.156	-12.1±2.3	10.63	96.93

Footnotes: PDI=polydispersity index, ZP=zeta potential, LC=loading content, EE=entrapment efficiency, n=3.

MP Biochemicals, Solon, OH). Centrosomes were stained with rabbit polyclonal anti-pericentrin antibody (AB4448, Abcam, Cambridge, MA) and rhodamine-conjugated goat anti-rabbit antibody (Cappel MP Biochemicals). Actin filaments were stained with rhodamine-conjugated phalloidin (Invitrogen, Carlsbad, CA). Cells were mounted with 4',6-diamidino-2-phenylindole (DAPI)-containing Prolong Gold (Invitrogen). Microscopy was performed on a spinning disc confocal microscope Olympus IX81 DSU under control of SlideBook software (Olympus, Tokyo, Japan).

Western blot

Compounds treated cancer samples were separated by SDS-PAGE were transferred to nitrocellulose membranes. After being blocked in 5% bovine serum albumin (w/v) at room temperature for 1 hr, the membranes were rinsed and incubated at 4°C overnight with primary anti-total and phosphorylated procaspase-3, -8 -9, β-actin antibody as well as related molecule antibodies (1:1000). The membranes were then washed and incubated with secondary antibody (1:2000~3000) at room temperature for 1 hr, developed with chemiluminescence ECL reagent (LumiGold, SignaGen) and exposed to Hyperfilm MP (GE Healthcare). Tumor samples were lysed in RIPA buffer (50 mM Tris-HCl, pH 7.5, 150 mM NaCl, 5 mM EDTA, 0.1% SDS, 0.5% sodium deoxycholate, 1% NP-40, supplemented with Complete Mini protease inhibitors) and equal amounts of protein were subjected to western blotting analysis.

Statistical methods

All experiments were performed at least 3 times unless otherwise mentioned. Student's t-test statistical analysis was carried out with SPSS 13.0 software, with $p < 0.05$ considered to indicate a significant difference.

Results

Size, surface morphology, zeta potential, and entrapment efficiency

Particle size and surface properties of the nanoparticles play a crucial role in drug release kinetics, cellular uptake behavior as well as in vivo pharmacokinetics and tissue distribution [19]. The particle size and size distribution of the maytansine-NPs were detected by dynamic light scattering (DLS) equipment and the data were displayed in **Table 1**. According to PDI, ZP (mV), Particle Size (nm), LC (%) and EE (%) parameters, star-shaped folate-core PLA-TPGS Copolymer nanoparticles displays perfect advantage for an efficient drug delivery vehicle. The physical properties of the maytansine-NPs were displayed in **Figure 1**. The average hydrodynamic size of the maytansine-NPs is approximately 120 nm in diameter, which is in the excellent size range for accumulating readily in tumor vasculature due to enhanced permeation and retention effects [20].

In vitro release profiles

The in vitro drug release profiles of the maytansine-NPs in PBS (pH 7.4) in the first 30 days are shown in **Figure 2**. The continuous release of drugs from the polymeric nanoparticles could occur either by diffusion of the drug from the polymer matrix or by the erosion of the polymer, which are affected by constituents and architectures of the polymers, surface erosion properties of the nanoparticles, and the physicochemical properties of the drugs [21]. The maytansine release from the linar-FA-PLA-TPGS nanoparticles and star-FA-PLA-TPGS nanoparticles displayed an initial burst of 37.2% and 40.4% in the first 3 days, respectively. The accumulative maytansine release in the first 30 days was found in the following order: star-FA-PLA-TPGS nanoparticles (65.5%) > linar-FA-PLA-TPGS nanoparticles (44.1%). The star-FA-PLA-TPGS nanoparticles displayed stable and high efficient drug release than the linear FA-PLA-TPGS nanoparticles when the copolymers had the same molecular weight.

Cellular uptake of fluorescent FA-PLA-TPGS nanoparticles

It has been demonstrated that the therapeutic effects of drug-loaded nanoparticles depend

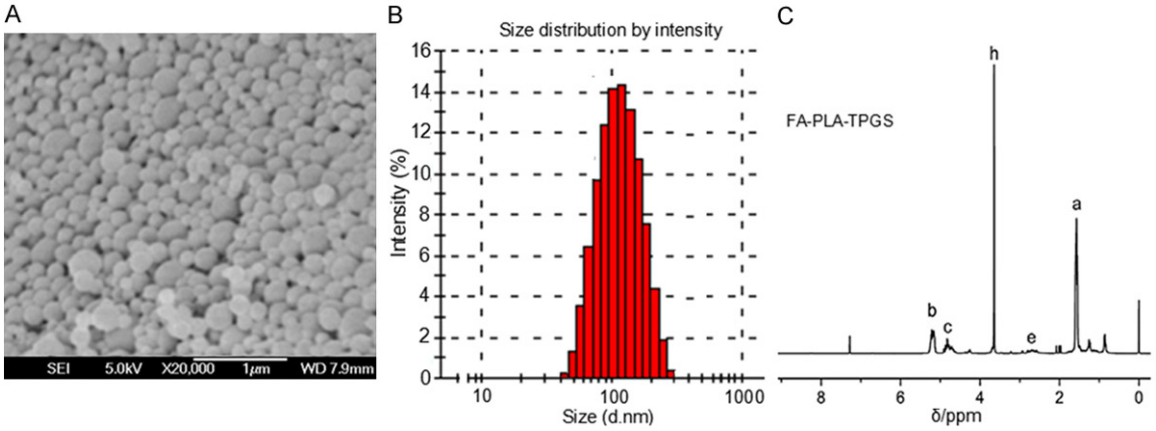

Figure 1. The physical properties of the star-shaped FA-PLA-TPGS nanoparticles. A. Zeta potential distribution of the star-shaped FA-PLA-TPGS nanoparticles; B. Size distribution of the star-shaped FA-PLA-TPGS nanoparticles detected by DLS; C. Typical ^{1}H NMR spectra of FA-PLA-TPGS copolymers.

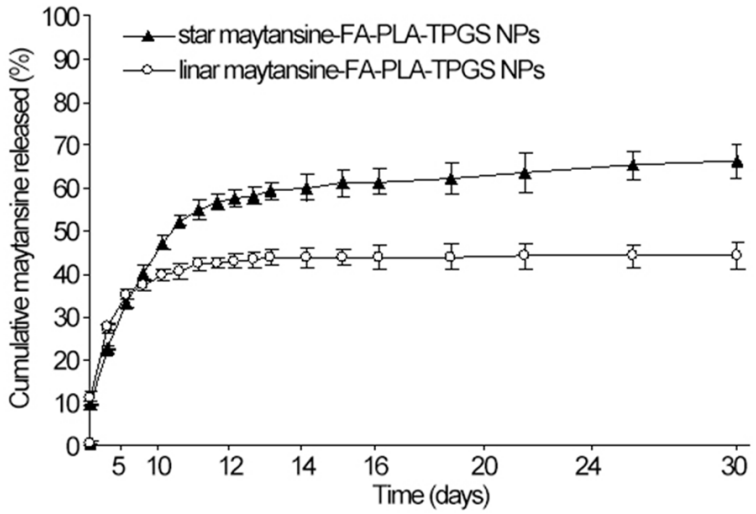

Figure 2. *In vitro* release profiles of the maytansine-loaded FA-PLA-TPGS nanoparticles (maytansine-NPs). Phosphate-buffered saline (PBS, containing 0.1% w/v Tween 80, pH 7.4) was selected as the release medium. The nanoparticle dispersion was put in an orbital shaker and shaken at 130 rpm at 37 °C. HPLC was performed to measure the released drug concentration.

on internalization and sustained retention of the nanoparticles by diseased cells [21]. Although the *in vitro* and *in vivo* biologic processes could be very different, an *in vitro* investigation may provide some preliminary evidence to show the advantages of nanoparticles. Coumarin-6 served as a fluorescent probe in an attempt to represent the drug in the nanoparticles for visualization and quantitative analysis of cellular uptake of the nanoparticles [8, 9]. **Figure 3** shows the images of tumor cells after determined time (12 h, 24 h and 36 h) of incubation with coumarin 6-loaded FA-PLA-TPGS nanoparticle dispersion in DMEM at the concentration of 250 nmol/L. It can be seen from this figure that, with the extension of the schedule, the green fluorescent in cells continuously enhanced, indicating that the fluorescent nanoparticles had been internalized into these SKBR3 cells.

In vitro sensitivity of breast cells to maytansine and maytansine-NPs

Next we compared the effects of maytansine and maytansine-NPs on SKBR3 cell lines in vitro. After 48 h and 72 h incubation respectively, maytansine-NPs and maytansine inhibited the growth of SKBR3 cells in a dose-dependent manner. The growth inhibition of maytansine-NPs was stronger compared with that of maytansine in the concentration range of 0.1-10.0 nmol/L ($p > 0.05$, n=3) (**Figure 4**).

Effects of maytansine-NPs on microtubule organization

To assess the effects of maytansine-NPs on the microtubule network, tumor cells were fixed and stained for microtubules, actin and chromatin and examined by Fluorescence microscopy. In control cells in interphase, microtu-

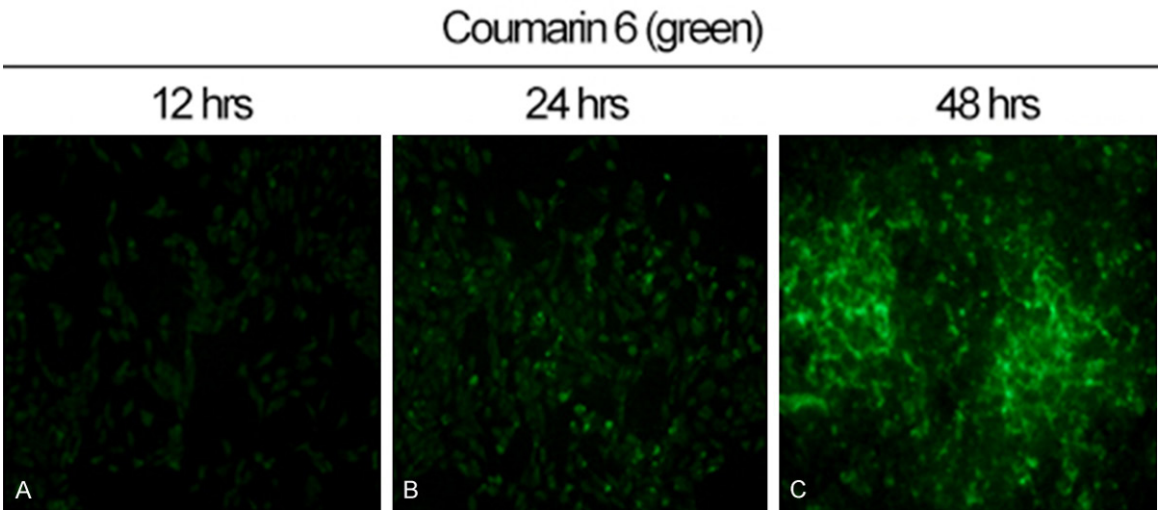

Figure 3. Fluorescence microscopy images images of SKBR3 after 4 h of incubation with the coumarin 6-loaded star FA-PLA-TPGS nanoparticles (coumarin 6-NPs). The coumarin 6-loaded nanoparticles were green (×100). A. SKBR3 cells incubated with coumarin 6-NPs for 12 hours; B. SKBR3 cells incubated with coumarin 6-NPs for 24 hours; C. SKBR3 cells incubated with coumarin 6-NPs for 36 hours.

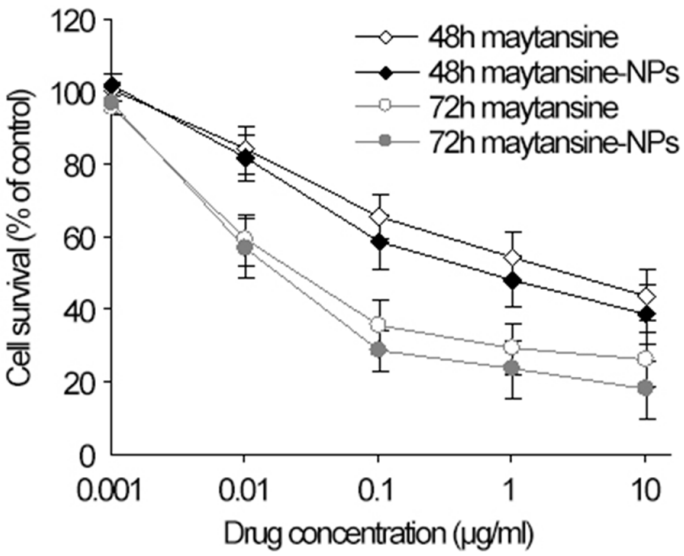

Figure 4. Growth inhibitory effects of maytansine and maytansine-NPs on SKBR3 cell lines in vitro. The effects of maytansine and maytansine-NPs (equivalent in maytansine) was tested at a concentrations 0.001, 0.01, 0.1, 1.0 and 10.0 nmol/L after treatment 48 h and 72 h, respectively. Both drug inhibited the growth of SKBR3 cells in a dose-dependent manner, but the effect on maytansine-NPs had no difference with that of maytansine in the concentration range of 0.01-10.0 nmol/L ($p > 0.05$).

bules formed a fine filamentous network throughout the cell and actin formed a filamentous network at the cell periphery (**Figure 5A**). After 24 h incubation with 0.01 nmol/L maytansine-NPs (equivalent in maytansine, follows the same) some interphase cells were slightly rounded, but the microtubules and actin fibers in these cells were indistinguishable from microtubules in control interphase cells (**Figure 5B**). At a maytansine-NPs concentration of 0.1 nmol/L the microtubules in interphase cells were shorter, fewer in number, and had a patchy distribution; small aggregates of tubulin were also apparent (**Figure 5C**). At 1.0 nmol/L maytansine-NPs microtubules rarely remained (**Figure 5D**). The actin fiber network was unchanged.

Effect of drug on the expression levels of apoptosis-related proteins

In order to study the effect of maytansine-NPs on the expression levels of apoptosis-related proteins, treatment with increasing concentrations of maytansine-NPs lasted for 48 h. Apoptosis body analyzed by fluorescence Microscopy shows that with increasing concentrations of drugs, apoptotic bodies were also increased. Western blot analysis was conducted to investigate the expression levels of procaspase-3, -8, -9, -10 and Bcl-2 proteins. It was found that following treatment with maytansine-NPs with increasing concentrations of drugs, the expression levels of breast cancer SKBR3 cell procaspase-3 and -9 proteins significantly declined (p

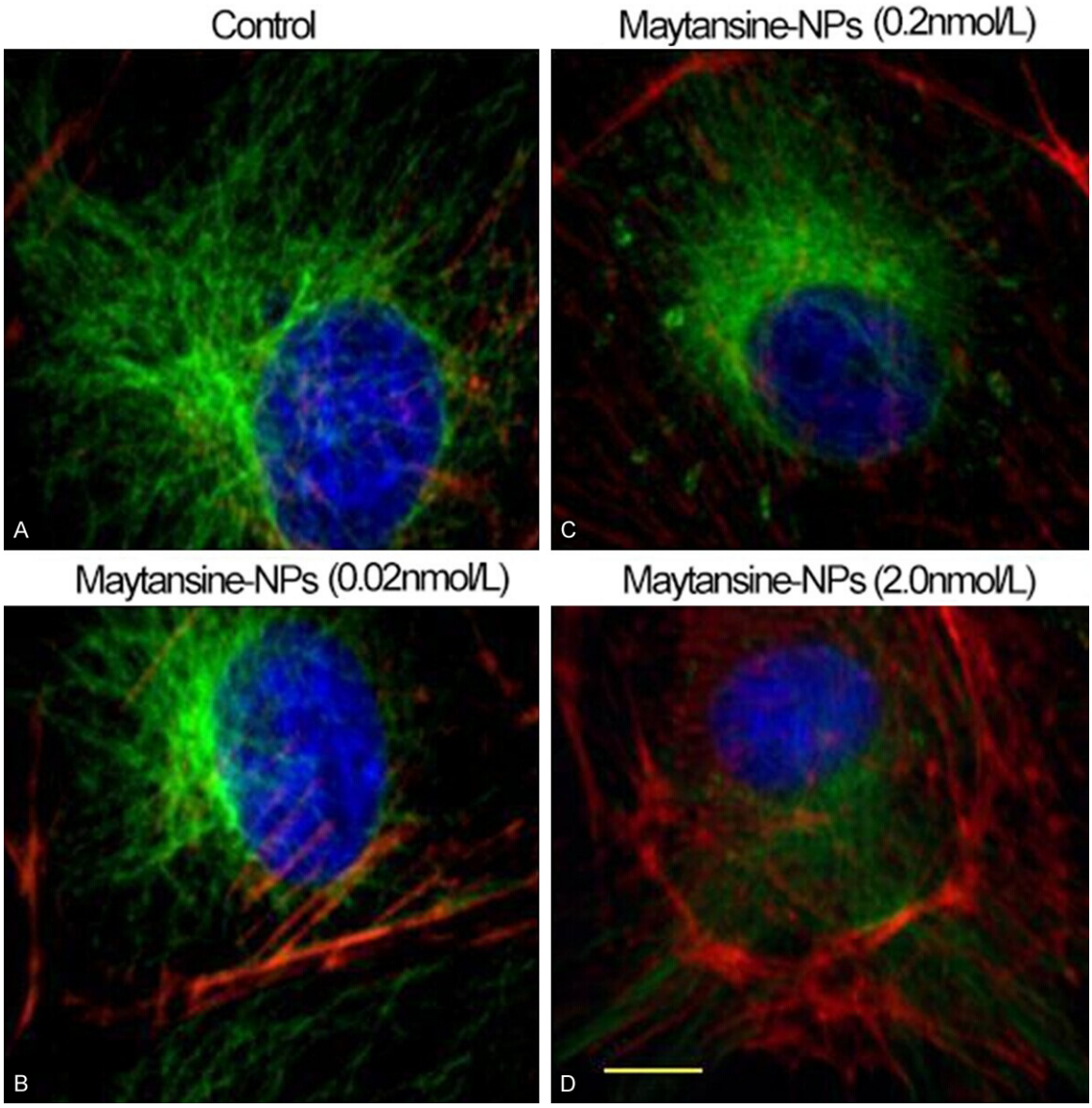

Figure 5. Effects of maytansine-NPs on microtubule organization in interphase and mitosis, tumor cells were fixed and stained for α-tubulin (green), actin (red) and DNA (blue). A. Control cells; B. Cells treated for 24 h with 0.02 nmol/L maytansine-NPs (equivalent in maytansine 0.01 nmol/L). C. Cells treated for 24 h with 0.2 nmol/L maytansine-NPs (equivalent in maytansine 0.1 nmol/L). D. Cells treated for 24 h with 2.0 nmol/L maytansine-NPs (equivalent in maytansine 1.0 nmol/L), all microtubules were depolymerized. Scale bar=5 μm.

< 0.05), while no significant differences were observed in the expression level of procaspase-8, -10 and Bcl-2 protein ($p > 0.05$). Our data demonstrated that maytansine and maytansine-NPs-induced SKBR3 apoptosis may occur through the mitochondria-mediated caspase-3 and -9 pathways.

Discussion

In vitro experiments showed that maytansine at very low concentrations can inhabit the growth of L1210, L1/5178 leukemia cells reversibly, and inhabit irreversibly at higher concentrations [22, 23]. *In vivo*, it can inhibit S180, L1210, P388, B16 melanoma, Lewis lung carcinoma, and other transplanted tumors through inhibiting the polymerization of tubulin, affecting microtubule formation, simultaneously inhibiting synthesis of DNA, RNA and protein [23, 24]. Therefore, maytansine is a strong potential anti-cancer drug, however, like all chemotherapy drugs, maytansine has some important adverse effects, such as bone marrow inhi-

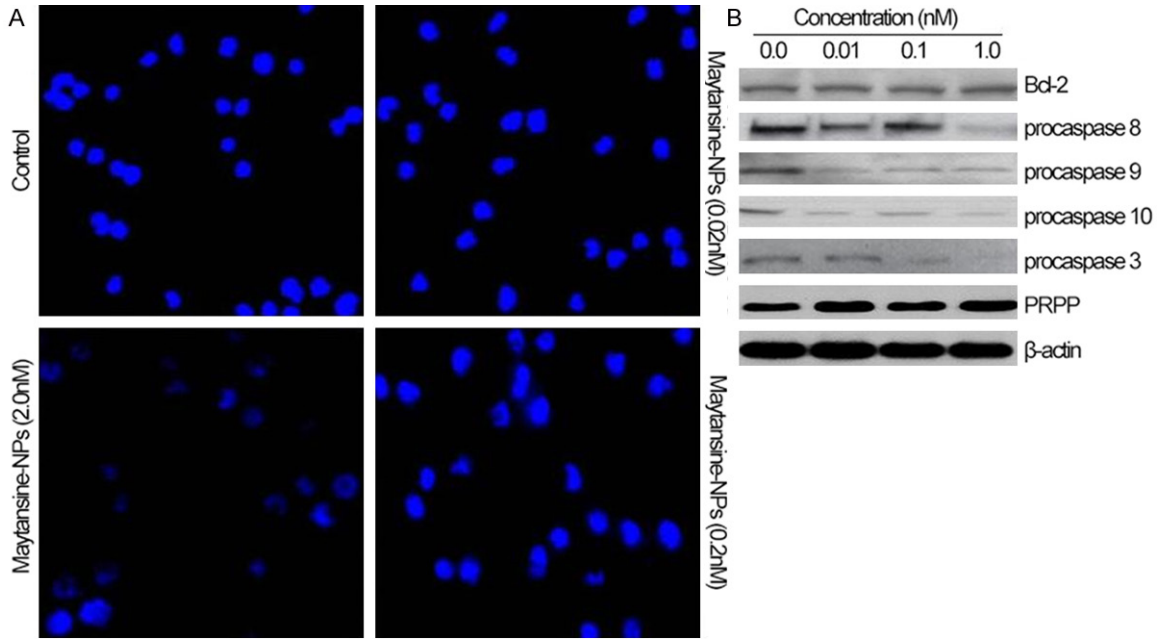

Figure 6. Induction of apoptosis by maytansine-NPs-mediated cytotoxicity. The cells were treated with increasing concentrations of maytansine-NPs for 48 h. A. Apoptosis body of the cells were incubated with DAPI, and then analyzed by fluorescence Microscopy; B. Western blot analysis was used to analyze the expression of procaspase-3, -8, -9, -10 and Bcl-2 proteins. The protein levels of procaspase-3, -9 and -10 were shown to decrease in drug concentration dependent manners by maytansine-NPs- induced apoptosis (equivalent in maytansine 0.00, 0.01, 0.1, and 1.0 nmol/L respectively).

bition, liver toxicity, gastrointestinal reactions, and permanent peripheral nerve damage occurring [24]. Therefore, novel therapeutic approaches are urgently needed to minimize untoward drug-related toxicities and ultimately enhance patient outcomes, which is critical to ongoing research. Nanomedicine has been suggested as a novel approach for the treatment of such tumors, offering potential for increased efficacy and reduced off-target cytotoxic effects [25].

In our previous research [8, 9], we have developed the star-shaped cholic acid-core PLA-TPGS (CA-PLA-TPGS) conjugate nanoparticles for nanoparticle formulation of small molecular anti-tumor drugs and characterized the property of the nanoparticle *in vitro*. In this current study, we have shown that maytansine can be successfully formulated into star-shaped folate-core PLA-TPGS (FA-PLA-TPGS) nanoparticles [9, 26]. These particles elicit improved cytotoxic effects over free drug maytansine toward human breast cancer cells, which is further enhanced by FA targeting, exploiting the FR that is frequently over-expressed in breast carcinomas.

To improve internalization using direct conjugation to FA targeting FR [27], Folate (FA), one of the most commonly used targeting moiety to specifically deliver nano-scaled systems to tumor cells, binds to its receptor-folate receptor (FR)- with a very high affinity (*K*D 0.1~1 nM [27]. The FA facilitated its uptake via receptor-mediated endocytosis and slowly releasing nanoparticles packaged drugs exert anti-tumor effects in the targeting tissue. We use FA targeting FR which is main expression of the surface of tumor cells, and use star-shaped FA-PLA-TPGS nanoparticle as drug carrier, for star-shaped FA-PLA-TPGS nanoparticles could achieve higher drug loading content and entrapment efficiency, resulting in faster drug release as well as higher cellular uptake and cytotoxicity [28]. The results shown here revealed that The FA-mediated maytansine-loaded star-shaped-core PLA-TPGS Copolymer nanoparticles (maytansine-NPs) formulations were fabricated by a modified nanoprecipitation procedure. The particle size of maytansine-NPs could be prepared favorably approximately 120 nm in diameter, maytansine-NPs has high cellular uptake and accumulate at the tumor site preferentially due

to the enhanced permeability and retention (EPR) effect, and hold more reasonable pharmacokinetics and more desirable biodistribution [29, 30].

In vitro studies, we found that maytansine-NPs inhibited proliferation of SKBR3 cells at subnanomolar or nanomolar concentrations in concert with mitotic arrest and suppression of microtubule dynamic instability indicating that the maytansine-NPs exert their superior antimitotic effects via a common mechanism involving suppression of microtubule dynamic instability. Moreover, We found that maytansine can mediate cell apoptosis, while at 0.1 to 10.0 nmol/L level, apoptosis-related molecular test results also demonstrated a significant increase in apoptosis of tumor cells (**Figure 6**).

So we think that maytansine-FA-PLA-TPGS nanoparticles (maytansine-NPs) can be targeted specifically to FR^+ cancer cells and promotes apoptosis of tumor cells, which has a potential to establish new treatment paradigms. Ongoing research is critical in improving maytansine-NPs drug concentration in the target tissue, reducing non-specific distribution, and promoting apoptosis of tumor cells *in vivo*. further optimization of targeting ability, versatile, practical, non-toxic, stable and development of efficient new drug carrier in order to minimise untoward drug-related toxicities and ultimately enhance patient outcomes.

Acknowledgements

The authors are grateful for the Open Research Fund Program of the State Key Laboratory of Virology of China (no.2014KF004), Guangdong Provincial Health Department Fund (no. A2011224), the science and technology supporting fund in Huai'an (HAS2013010), the startup funds in science research from Huai'an Second People's Hospital (YK201217), the National High Technology Research and Development Program (863 Program) (no. 2011AA02A111), and 2011 Infectious Disease Prevention and Control Technology major project (no. 2012ZX10004903).

Disclosure of conflict of interest

None to declare.

Address correspondence to: Hong Dai, Department of Clinical Laboratory, Medical College, Hunan Normal University, Changsha 410006, Hunan, China. E-mail: hdtxl_2014@163.com; Deqiang Li, Department of Integrated Internal Medicine, The First Affiliated Hospital of Zhejiang University, Hangzhou 310003, China. E-mail: lideqiangdoc@163.com

References

[1] Vacchelli E, Aranda F, Eggermont A, Galon J, Sautes-Fridman C, Cremer I, Zitvogel L, Kroemer G and Galluzzi L. Trial Watch: Chemotherapy with immunogenic cell death inducers. Oncoimmunology 2014; 3: e27878.

[2] Cadossi R, Ronchetti M and Cadossi M. Locally enhanced chemotherapy by electroporation: clinical experiences and perspective of use of electrochemotherapy. Future Oncol 2014; 10: 877-890.

[3] Patel KC, Hageman K and Cooper MR. Ado-trastuzumab emtansine for the treatment of human epidermal growth factor receptor 2-positive metastatic breast cancer. Am J Health Syst Pharm 2014; 71: 537-548.

[4] Jean DC, Baas PW and Black MM. A novel role for doublecortin and doublecortin-like kinase in regulating growth cone microtubules. Hum Mol Genet 2012; 21: 5511-5527.

[5] Delphin C, Bouvier D, Seggio M, Couriol E, Saoudi Y, Denarier E, Bosc C, Valiron O, Bisbal M, Arnal I and Andrieux A. MAP6-F is a temperature sensor that directly binds to and protects microtubules from cold-induced depolymerization. J Biol Chem 2012; 287: 35127-35138.

[6] Hawkins TL, Sept D, Mogessie B, Straube A and Ross JL. Mechanical properties of doubly stabilized microtubule filaments. Biophys J 2013; 104: 1517-1528.

[7] Kim JH, Choi AR, Kim YK and Yoon S. Co-treatment with the anti-malarial drugs mefloquine and primaquine highly sensitizes drug-resistant cancer cells by increasing P-gp inhibition. Biochem Biophys Res Commun 2013; 441: 655-660.

[8] Xue M and Zink JI. Probing the Microenvironment in the Confined Pores of Mesoporous Silica Nanoparticles. J Phys Chem Lett 2014; 5: 839-842.

[9] Tang X, Cai S, Zhang R, Liu P, Chen H, Zheng Y and Sun L. Paclitaxel-loaded nanoparticles of star-shaped cholic acid-core PLA-TPGS copolymer for breast cancer treatment. Nanoscale Res Lett 2013; 8: 420.

[10] Henne WA, Kularatne SA, Hakenjos J, Carron JD and Henne KL. Synthesis and activity of a folate targeted monodisperse PEG camptothecin conjugate. Bioorg Med Chem Lett 2013; 23: 5810-5813.

[11] Vlashi E, Kelderhouse LE, Sturgis JE and Low PS. Effect of folate-targeted nanoparticle size on their rates of penetration into solid tumors. ACS Nano 2013; 7: 8573-8582.
[12] Tan GR, Feng SS and Leong DT. The reduction of anti-cancer drug antagonism by the spatial protection of drugs with PLA-TPGS nanoparticles. Biomaterials 2014; 35: 3044-3051.
[13] Gan CW and Feng SS. Transferrin-conjugated nanoparticles of poly(lactide)-D-alpha-tocopheryl polyethylene glycol succinate diblock copolymer for targeted drug delivery across the blood-brain barrier. Biomaterials 2010; 31: 7748-7757.
[14] Haddley K. Trastuzumab emtansine for the treatment of HER2-positive metastatic breast cancer. Drugs Today (Barc) 2013; 49: 701-715.
[15] Zhang Z, Lee SH, Gan CW and Feng SS. In vitro and in vivo investigation on PLA-TPGS nanoparticles for controlled and sustained small molecule chemotherapy. Pharm Res 2008; 25: 1925-1935.
[16] Beck A, Senter P and Chari R. World Antibody Drug Conjugate Summit Europe: February 21-23, 2011; Frankfurt, Germany. MAbs 2011; 3: 331-337.
[17] Lopez-Avila V, Cooley J, Urdahl R and Thevis M. Determination of stimulants using gas chromatography/high-resolution time-of-flight mass spectrometry and a soft ionization source. Rapid Commun Mass Spectrom 2012; 26: 2714-2724.
[18] Lu L, Zhang L, Wai MS, Yew DT and Xu J. Exocytosis of MTT formazan could exacerbate cell injury. Toxicol In Vitro 2012; 26: 636-644.
[19] Guo O, Li X, Yang Y, Wei J, Zhao Q, Luo F and Qian Z. Enhanced 4T1 breast carcinoma anticancer activity by co-delivery of doxorubicin and curcumin with core-shell drug-carrier based on heparin modified poly(L-lactide) grafted polyethylenimine cationic nanoparticles. J Biomed Nanotechnol 2014; 10: 227-237.
[20] Zhou H, Stafford JH, Hallac RR, Zhang L, Huang G, Mason RP, Gao J, Thorpe PE and Zhao D. Phosphatidylserine-targeted molecular imaging of tumor vasculature by magnetic resonance imaging. J Biomed Nanotechnol 2014; 10: 846-855.
[21] Patel MD, Date PV, Gaikwad RV, Samad A, Malshe VC and Devarajan PV. Comparative evaluation of polymeric nanoparticles of rifampicin comprising Gantrez and poly(ethylene sebacate) on pharmacokinetics, biodistribution and lung uptake following oral administration. J Biomed Nanotechnol 2014; 10: 687-694.
[22] Nakao H, Senokuchi K, Umebayashi C, Kanemaru K, Masuda T, Oyama Y and Yonemori S. Cytotoxic activity of maytanprine isolated from Maytenus diversifolia in human leukemia K562 cells. Biol Pharm Bull 2004; 27: 1236-1240.
[23] Chu YW and Polson A. Antibody-drug conjugates for the treatment of B-cell non-Hodgkin's lymphoma and leukemia. Future Oncol 2013; 9: 355-368.
[24] Sapra P, Betts A and Boni J. Preclinical and clinical pharmacokinetic/pharmacodynamic considerations for antibody-drug conjugates. Expert Rev Clin Pharmacol 2013; 6: 541-555.
[25] Barahuie F, Hussein MZ, Fakurazi S and Zainal Z. Development of drug delivery systems based on layered hydroxides for nanomedicine. Int J Mol Sci 2014; 15: 7750-7786.
[26] Gaillard J, Ramabhadran V, Neumanne E, Gurel P, Blanchoin L, Vantard M and Higgs HN. Differential interactions of the formins INF2, mDia1, and mDia2 with microtubules. Mol Biol Cell 2011; 22: 4575-4587.
[27] Benchaala I, Mishra MK, Wykes SM, Hali M, Kannan RM and Whittum-Hudson JA. Folate-functionalized dendrimers for targeting Chlamydia-infected tissues in a mouse model of reactive arthritis. Int J Pharm 2014; 466: 258-265.
[28] Tomasina J, Poulain L, Abeilard E, Giffard F, Brotin E, Carduner L, Carreiras F, Gauduchon P, Rault S and Malzert-Freon A. Rapid and soft formulation of folate-functionalized nanoparticles for the targeted delivery of tripentone in ovarian carcinoma. Int J Pharm 2013; 458: 197-207.
[29] Ali T, Nakajima T, Sano K, Sato K, Choyke PL and Kobayashi H. Dynamic fluorescent imaging with indocyanine green for monitoring the therapeutic effects of photoimmunotherapy. Contrast Media Mol Imaging 2014; 9: 276-282.
[30] Upreti M, Jyoti A and Sethi P. Tumor microenvironment and nanotherapeutics. Transl Cancer Res 2013; 2: 309-319.